

Tool *QUATTRO-20* for Examining of the Recurrent Sequencies Generated by Discrete Analogue of the Verhulst Equation

Jelena Kozmina*, Alytis Gruodis

Department of IT Technologies, Vilnius Business College, Kalvarijų g. 129-401, LT-08221 Vilnius, Lithuania

* Corresponding author, e-mail: Jelena.Kozmina@gmail.com

Received: 16 April 2023
 Accepted: 30 May 2023
 Online: 30 June 2023

JEL: C25; C62; C63, C73.

Abstract. *QUATTRO-20* as advanced tool for estimation of the recurrent sequences was created and tested. Discrete analogue of Verhulst equation $x_{t+1}=F(x_t)$, $F(x)=rx(1-x)$, $t=0, 1, 2, \dots$, was selected as the model of recurrent sequence. Related mathematical material is presented in user-friendly form: convergence conditions, Lyapunov index, behaviour of the sequencies generated by second, third, fourth compositions of function $F(x)$. *QUATTRO-20* contains several visualization methods such as xy plot, Bifurcation diagram, distribution of Lyapunov index, CobWeb plot, graphical solution. Novel graphical technique of realization of the sequence convergence was presented.

Keywords: Discrete analogue of Verhulst equation; Logistic map; convergence condition; Bifurcation diagram; Lyapunov exponent; Lyapunov index; CobWeb plot.

Citation: Jelena Kozmina, Alytis Gruodis (2023) Tool *QUATTRO-20* for Examining of the Recurrent Sequencies Generated by Discrete Analogue of the Verhulst Equation . – *Applied Business: Issues & Solutions* 1(2023)16–29 – ISSN 2783-6967.

<https://doi.org/10.57005/ab.2023.1.3>

Introduction

Stochastic processes are present in many fields of biology (population dynamics, host-parasite interactions), sociology (growth of population), economics (market activity), cryptography, steganography etc. [1,2]. For population dynamics, there is never enough information to understand fully a population amount and dynamics of the surrounding influence (affection) [3]. This means that contemporary modeling emphasizes uncertainty by incorporating stochasticity [3,4]. In many cases, stochastic behaviour is very complicated, and unique non-trivial solutions could be reached in approximate form, using for example entropy approach [5] only. As Bertel et al [6] pointed out, chaotic phenomena can appear in many dynamical systems which could be characterized by following conditions: non-linear behaviour and evolution progress (as expression of recursive nature). Historical overview of dynamical progress problem made by Bacaer [7] contains several fields, in particular, pandemic activity [8], meteorological approach [9], predator–prey system etc.

Large number of different dynamic systems could be described using recurrence relations [10]. Possibility to define the rule-based sequence allows us generate the following term as a function of the previous term. From large set of recurrence relations, one of the classical examples [7] is well-known *Logistic equation* or *Verhulst equation*

$$x' = r \cdot x \cdot (1 - x). \quad (1)$$

Discrete form of Logistic equation (*Discrete analogue of Verhulst equation*, also *Logistic map*) allows to generate the sequence of terms as the function of the preceding terms for certain population analysis:

$$x_{t+1} = r \cdot x_t \cdot (1 - x_t), \quad t = 0, 1, 2, \dots, \quad (2)$$

where x_t represents the current term and parameter $r > 0$ represents the coefficient of proportionality characterizing, for example, the rate of population growth [10-11].

Evolution of physical/social/biological systems must be estimated in the framework of convergence behaviour, and primary importance of such task is related to obtaining the various dynamical regimes of the certain system.

For functional generated behaviours, several mathematical techniques could be used for visualization of sets, estimation of evolution types, next-step prognosis and future guessing.

Firstly, xy or xyz plot of generated sets allows us to establish the character of distribution: attracting or chaotic behaviour [12-13]. Secondly, the bifurcation diagram shows the values to which the sequence asymptotically approaches depending on the parameter (fixed points, periodic orbits or chaotic attractors) [14, 10]. Thirdly, xy graphical distribution generated as the CobWeb Plot corresponds to Bifurcation diagram. Fourthly, distribution of Lyapunov index allows to establish the critical points of reswitching between regimes [15-16]. Present operations require exact generation of items and representation according to all requested parameters.

This work is devoted to describing the functional possibilities of the advanced tool *QUATTRO-20* [17] which was created for teaching purposes to explore Discrete analogue of Verhulst equation in user-friendly manner:

- 1) to plot Bifurcation diagram;
- 2) to plot the map for first derivative of first, second, third and fourth compositions of $F(x)$;
- 3) to plot distribution of Lyapunov index;
- 4) to plot CobWeb plot;
- 5) to solve $x=F(x)$ graphically.
- 6) to generate a recurrent sequence of requested amount.

1. Description of dynamic system

According to Eq.(2), Discrete analogue of Verhulst equation or logistic map represents quadratic function $F(x)$ at certain r :

$$F(x) = r \cdot x \cdot (1 - x), \quad (3)$$

when $r \in (0;4)$ [11,7]. Historically, this is perhaps the most studied function. For standard growth model, different approaches could be used starting from classical [7] up to more complicated. For example, Kalman [13] presented a solution of Discrete analogue of Verhulst equation using matrix algebra technique.

1.1. Convergence behaviour of dynamic system

In mathematics, a fixed point of a function is an element of the function's domain that is mapped to itself by the function. Accordingly, x^* is a fixed point of the function $F(x)$ if

$$F(x^*) = x^*. \quad (4)$$

Let us express the second composition F^2 :

$$F^2(x) = F(F(x)), \quad (5)$$

third composition F^3 ,

$$F^3(x) = F(F(F(x))), \dots, \quad (6)$$

n -th composition F^n ,

$$F^n(x) = F(F^{n-1}(x)), \quad n = 3, 4, \dots. \quad (7)$$

Do not get confused because notation $F^2(x)$ means the composition according to Eq.(5) but not square of $F(x)$.

Using fixed point notation,

$$F^2(x^*) = F(F(x^*)) = F(x^*) = x^*, \quad (8)$$

$$F^3(x^*) = F(F^2(x^*)) = F(x^*) = x^*. \quad (9)$$

It follows that

$$F^n(x^*) = x^*, \quad n = 2, 3, \dots. \quad (10)$$

We use this fact when discussing the fixed points of the equation:

$$x = F^n(x), \quad n = 2, 3, \dots. \quad (11)$$

Note that the set of fixed points of the function $F(x)$ is contained in the set of fixed points of the function $F^2(x)$, and the set of fixed points of the function $F^{n-1}(x)$ is contained in the set of fixed points of the function $F^n(x)$, $n=3, 4, \dots$.

Convergence condition. Let's consider the equation

$$x = F(x). \quad (12)$$

Function F is a contracting map in a closed interval $I \in \mathbb{R}$ if F meets two following conditions.

1. $F: I \rightarrow I$, where I is a closed interval. If $x \in I$, then $F(x) \in I$.
2. F is the contraction on this interval. It means that some $L \in (0;1)$ exists, such that inequality

$$|F(x) - F(x')| \leq L \cdot |x - x'| \quad (13)$$

is valid for any $x, x' \in I$.

Then, according to the contraction mapping principle, for any initial value $x_0 \in I$, the sequence (x_t) , $t=0, 1, 2, \dots$, defined by the condition $x_{t+1}=F(x_t)$, converges to the value x^* such, that $x^*=F(x^*)$. It means that x^* is a solution of equation $x=F(x)$. Whether the sequence (x_t) converges to x^* or not depends on the value of $F'(x)|_{x=x^*}$. Condition 2 will be done, if

$$|F'(x)|_{x=x^*} < 1. \quad (14)$$

If for sufficiently large numbers t the members of the sequence (x_t) are close enough to a point x^* , then the point x^* attracts this sequence, and x^* is an attractor.

1.2. Attractors

In [11], a Discrete analogue of the Verhulst equation

$$x_{t+1} = r \cdot x_t \cdot (1 - x_t), \quad t = 0, 1, 2, \dots, \quad (15)$$

was considered and several results related to the convergence were discussed. This is a special case of the sequence

$$x_{t+1} = F(x_t) \quad (16)$$

where

$$F(x) = rx(1 - x). \quad (17)$$

We have studied Eq.(15) for various values of the parameter r in interval $[0;4]$ [11]. Initially, we have considered the sequence Eq.(16) and solved following equation:

$$x = F(x). \quad (18)$$

To do this, we passed to the limit in Eq.(15), found the exact solutions of equation

$$x = r \cdot x \cdot (1 - x) \quad (19)$$

and then explored them.

Two solutions of Eq.(19) are presented below:

$$x_1^* = 0, \quad x_2^* = \frac{r-1}{r}. \tag{20}$$

These two points become the attractor if following condition is satisfied:

$$\left| \frac{dF(x)}{dx} \Big|_{x=x_{1,2}^*} \right| < 1, \tag{21}$$

where

$$\frac{dF(x)}{dx} = r - 2rx. \tag{22}$$

For first solution x_1^*

$$\frac{dF(x)}{dx} \Big|_{x=x_1^*} = r, \tag{23}$$

$$|r| < 1. \tag{24}$$

The solution x_1^* is the fixed point attractor for $0 < r < 1$.

For second solution x_2^*

$$\frac{dF(x)}{dx} \Big|_{x=x_2^*} = 2 - r, \tag{25}$$

$$|2 - r| < 1. \tag{26}$$

The solution x_2^* is the fixed point attractor for $1 < r < 3$. Detail analysis and explanations are presented in [11, 6, 18].

For interval $3 < r < 4$ we have considered the sequence

$$x_{t+2} = F(x_{t+1}) = F(F(x_t)) = F^2(x_t) \tag{27}$$

and solved the equation

$$x = F^2(x) \tag{28}$$

when

$$F^2(x) = r^2x(1 - (r+1)x + 2rx^2 - rx^3). \tag{29}$$

To do this, we passed to the limit in Eq.(27), found the exact solutions of equation

$$x = r^2x(1 - (r+1)x + 2rx^2 - rx^3) \tag{30}$$

and then explored them.

We got two additional solutions [11]:

$$x_{3,4}^{*(2)} = \frac{1+r \pm \sqrt{r^2-2r-3}}{2r}. \tag{31}$$

These two points become the periodic attractor if following condition is satisfied:

$$\left| \frac{dF^2(x)}{dx} \Big|_{x=x_{3,4}^{*(2)}} \right| < 1, \tag{32}$$

where

$$\frac{dF^2(x)}{dx} = r^2(1 - 2(r+1)x + 6rx^2 - 4rx^3). \tag{33}$$

In [11], an example of Discrete analogue of Verhulst equation was presented and discussed. Behaviour of the first derivative of $F^2(x)$ with respect to x at the points $x_{3,4}^{*(2)}$ was estimated numerically when $r=3.4$ using approximate values. In present work, mentioned situation is supplemented with calculations in a general form.

Calculating the expression of first derivative of $F^2(x)$ with respect to x

$$\frac{dF^2(x)}{dx} = r^2(1 - 2(r+1)x + 6rx^2 - 4rx^3) \tag{34}$$

at the points

$$x_3^{*(2)} = \frac{1+r + \sqrt{r^2-2r-3}}{2r}, \quad x_4^{*(2)} = \frac{1+r - \sqrt{r^2-2r-3}}{2r}, \tag{35}$$

we get

$$\frac{dF^2(x)}{dx} \Big|_{x=x_{3,4}^{*(2)}} = r^2 \left(1 - 2(r+1) \left(\frac{r+1 \pm \sqrt{r^2-2r-3}}{2r} \right) + 6r \left(\frac{r+1 \pm \sqrt{r^2-2r-3}}{2r} \right)^2 - 4r \left(\frac{r+1 \pm \sqrt{r^2-2r-3}}{2r} \right)^3 \right) = \tag{36}$$

$$= r^2 - (r^2+r)(1+r \pm \sqrt{r^2 - 2r - 3}) + 3(r^2+r)(r-1 \pm \sqrt{r^2 - 2r - 3}) - (1+r)(r \pm \sqrt{r^2 - 2r - 3}) + 1)(r \pm \sqrt{r^2 - 2r - 3}) - 1) = \quad (37)$$

$$= r^2 - (r^2 + r)(1 + r \pm \sqrt{r^2 - 2r - 3}) + 3(r^2 + r)(r - 1 \pm \sqrt{r^2 - 2r - 3}) - (1 + r)(2r^2 - 2r - 4 \pm 2r\sqrt{r^2 - 2r - 3}) = \quad (38)$$

$$= r^2 - \left(r(1+r)^2 \pm (r^2+r)\sqrt{r^2-2r-3} \right) + 3(r^2+r)(r-1) \pm 3(r^2+r)\sqrt{r^2-2r-3} - \left((1+r)(2r^2-2r-4) \pm 2(r^2+r)\sqrt{r^2-2r-3} \right) = r^2 - r(1+r)^2 + 3(r^2+r)(r-1) - (1+r)(2r^2-2r-4) = -r^2 + 2r + 4. \quad (39)$$

Interestingly, the result for both points $x_3^{*(2)}$ and $x_4^{*(2)}$ is the same:

$$\left. \frac{dF^2(x)}{dx} \right|_{x=x_{3,4}^{*(2)}} = -r^2 + 2r + 4. \quad (40)$$

To find out for which r the condition

$$\left| \left. \frac{dF^2(x)}{dx} \right|_{x=x_{3,4}^{*(2)}} \right| < 1 \quad (41)$$

is satisfied, we need to solve quadratic inequality

$$|-r^2 + 2r + 4| < 1. \quad (42)$$

Solution of Ineq.(42):

$$\begin{cases} r^2 - 2r - 4 < 1 \\ r^2 - 2r - 4 > -1 \end{cases} \Leftrightarrow \begin{cases} r^2 - 2r - 5 < 0 \\ r^2 - 2r - 3 > 0 \end{cases} \Leftrightarrow \begin{cases} r \in (1 - \sqrt{6}; 1 + \sqrt{6}) \\ r \in (-\infty; -1) \cup (+3; +\infty) \end{cases} \Leftrightarrow r \in (1 - \sqrt{6}; -1) \cup (3; 1 + \sqrt{6}). \quad (43)$$

In our case $r > 0$ then Ineq.(41) is satisfied if $r \in (3; 1 + \sqrt{6})$. Both solutions $x_3^{*(2)}$ and $x_4^{*(2)}$ are the periodic attractors for $3 < r < 1 + \sqrt{6}$.

Note that in partial case, when $r = 3.4$, there are four points of intersections of the graph of the function $F^2(x)$ with the line $y = x$:

$$x_1^* = 0, \quad x_2^* = \frac{12}{17} \approx 0.706, \quad x_3^* = \frac{1}{17}(11 - \sqrt{11}) \approx 0.452, \quad x_4^* = \frac{1}{17}(11 + \sqrt{11}) \approx 0.842. \quad (44)$$

Graphical solution of Eq.(30) is presented on Fig. 1: $y = x$ and $y = F^2(x)$ for $r = 3.4$, where

$$F^2(x) = 11.56x(-3.4x^3 + 6.8x^2 - 4.4x + 1). \quad (45)$$

Tangents at points of intersection at x_3^* and x_4^* are parallel.

Fig. 2 represents the Bifurcation diagram for interval $0 < r < 1 + \sqrt{6}$ constructed from functional expressions of x^* . For exact expressions, Eq.(20), Eq.(35) were used. Period-doubling point is presented at $r = 3.0$. Note, that $3.44948974278 < 1 + \sqrt{6} < 3.45$.

Further we need exact expression for functions $F^3(x)$ and $F^4(x)$ and for derivatives of these functions. Let us calculate the $F^3(x)$ as $F^2(F(x)) = F^2(rx - rx^2)$:

$$F^3(x) = r^2(rx - rx^2) - r^3(rx - rx^2)^2 - r^2(rx - rx^2)^2 + 2r^3(rx - rx^2)^3 - r^3(rx - rx^2)^4 \quad (46)$$

or in the form convenient for calculating the derivative

$$F^3(x) = -r^7x^8 + 4r^7x^7 - 2r^6(3r+1)x^6 + 2r^6(2r+3)x^5 - r^4(r^3+6r^2+r+1)x^4 + 2r^4(r^2+r+1)x^3 - r^3(r^2+r+1)x^2 + r^3x. \quad (47)$$

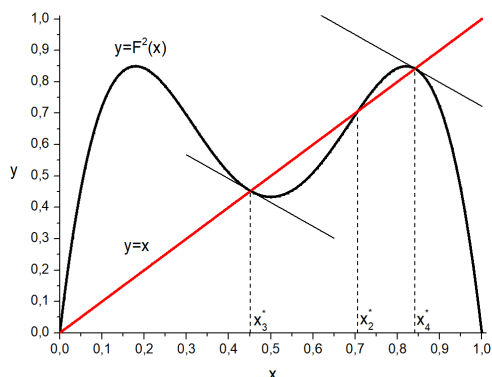


Fig. 1. $y = x$ and $y = F^2(x)$ for $r = 3.4$. Graphical solution of Eq.(30).

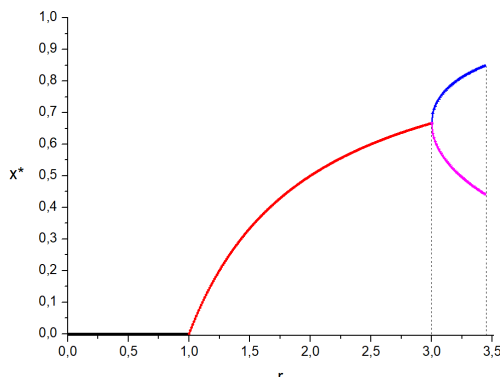


Fig. 2. Dependence of the attractor points x^* on parameter r , $r \in (0; 1 + \sqrt{6})$. Bifurcation diagram. Period-doubling point at $r = 3.0$.

The function $F^3(x)$ can also be written as a factorization:

$$F^3(x) = r^3x(1-x)(rx^2 - rx + 1)(r^3x^4 - 2r^3x^3 + r^2(r+1)x^2 - r^2x + 1). \tag{48}$$

Now we can calculate the derivative of $F^3(x)$:

$$\frac{dF^3(x)}{dx} = -8r^7x^7 + 28r^7x^6 - 12r^6(3r+1)x^5 + 10r^6(2r+3)x^4 - 4r^4(r^3+6r^2+r+1)x^3 + 6r^4(r^2+r+1)x^2 - 2r^3(r^2+r+1)x + r^3. \tag{49}$$

Function $F^4(x)$ can be calculated as $F^3(F(x))=F^3(rx - rx^2)$:

$$F^4(x) = -r^7(rx - rx^2)^8 + 4r^7(rx - rx^2)^7 - 2r^6(3r + 1)(rx - rx^2)^6 + 2r^6(2r + 3)(rx - rx^2)^5 - r^4(r^3 + 6r^2 + r + 1)(rx - rx^2)^4 + 2r^4(r^2 + r + 1)(rx - rx^2)^3 - r^3(r^2 + r + 1)(rx - rx^2)^2 + r^3(rx - rx^2). \tag{50}$$

$F^4(x)$ represents the sixteenth-order polynomial with respect to x :

$$\begin{aligned} F^4(x) = & -r^{15}x^{16} + 8r^{15}x^{15} - 4r^{14}(1 + 7r)x^{14} + 28r^{14}(1 + 2r)x^{13} - 2r^{12}(1 + 3r + 42r^2 + 35r^3)x^{12} + \\ & + 4r^{12}(3 + 9r + 35r^2 + 14r^3)x^{11} - 2r^{11}(3 + 17r + 45r^2 + 70r^3 + 14r^4)x^{10} + \\ & + 2r^{11}(15 + 30r + 60r^2 + 42r^3 + 4r^4)x^9 - r^8(1 + r + 6r^2 + 61r^3 + 70r^4 + 90r^5 + 28r^6 + r^7)x^8 + \\ & + 4r^8(1 + r + 6r^2 + 16r^3 + 13r^4 + 9r^5 + r^6)x^7 - 2r^7(1 + 4r + 4r^2 + 18r^3 + 18r^4 + 11r^5 + 3r^6)x^6 + \\ & + 2r^7(3 + 5r + 5r^2 + 12r^3 + 5r^4 + 2r^5)x^5 - r^5(1 + r + 7r^2 + 7r^3 + 7r^4 + 6r^5 + r^6)x^4 + \\ & + 2r^5(1 + r + 2r^2 + r^3 + r^4)x^3 - r^4(1 + r + r^2 + r^3)x^2 + r^4x \end{aligned} \tag{51}$$

Now we can calculate the derivative of $F^4(x)$:

$$\begin{aligned} \frac{dF^4(x)}{dx} = & -16r^{15}x^{15} + 120r^{15}x^{14} - 56r^{14}(1 + 7r)x^{13} + 364r^{14}(1 + 2r)x^{12} - 24r^{12}(1 + 3r + 42r^2 + 35r^3)x^{11} + \\ & + 44r^{12}(3 + 9r + 35r^2 + 14r^3)x^{10} - 20r^{11}(3 + 17r + 45r^2 + 70r^3 + 14r^4)x^9 + 18r^{11}(15 + 30r + 60r^2 + 42r^3 + 4r^4)x^8 - \\ & - 8r^8(1 + r + 6r^2 + 61r^3 + 70r^4 + 90r^5 + 28r^6 + r^7)x^7 + 28r^8(1 + r + 6r^2 + 16r^3 + 13r^4 + 9r^5 + r^6)x^6 - \\ & - 12r^7(1 + 4r + 4r^2 + 18r^3 + 18r^4 + 11r^5 + 3r^6)x^5 + 10r^7(3 + 5r + 5r^2 + 12r^3 + 5r^4 + 2r^5)x^4 - \\ & - 4r^5(1 + r + 7r^2 + 7r^3 + 7r^4 + 6r^5 + r^6)x^3 + 6r^5(1 + r + 2r^2 + r^3 + r^4)x^2 - 2r^4(1 + r + r^2 + r^3)x + r^4 \end{aligned} \tag{52}$$

The Discrete Analogue of the Verhulst equation (Eq.(15)) is interesting due to the following circumstances: for mentioned sequence at different values of the parameter r , a set of different attractors (fixed point attractor, periodic attractor, chaotic attractor) could be obtained. Methodologically, modelling tasks constructed by means of mentioned equation enable to understand the chaotic behaviour in real complicated forms of global complexity [19]. To analyse the behaviour of the sequence, a wide mathematic apparatus is used. Understanding the processes is facilitated using graphic dependencies.

It is necessary to point out that chaotic behaviour of the model system corresponding to the real system depends on the method precision [4]. Sensitivity of the model on initial conditions requires the detailed analysis of the stationary as well as dynamic behaviour.

1.3. Index of Lyapunov exponent

Schuster [20] uses Lyapunov spectrum for the system with many degrees of freedom. Many exponents express the sensitivity of the system with respect to different modes.

We consider the sequence

$$x_{t+1} = F(x_t), \quad t = 0, 1, 2, \dots, \tag{53}$$

where $F(x)=rx(1-x)$. Requested sequence could be written as $x_0, x_1, x_2, x_3, \dots, x_t, \dots$, where

$$x_1 = F(x_0), \tag{54}$$

$$x_2 = F(x_1) = F(F(x_0)) = F^2(x_0), \tag{55}$$

$$x_3 = F(x_2) = F(F(F(x_0))) = F^3(x_0), \dots, \tag{56}$$

$$x_t = F(x_{t-1}) = F^t(x_0). \tag{57}$$

At a closely adjacent point $(x_0+\varepsilon)$, we construct a similar sequence

$$x_0 + \varepsilon, F(x_0 + \varepsilon), F^2(x_0 + \varepsilon), F^3(x_0 + \varepsilon), \dots, F^t(x_0 + \varepsilon), \dots. \tag{58}$$

Let's introduce an average coefficient $e^{\lambda(x_0)}$, which shows how the distance between points changes in one iteration. Here $\lambda(x_0)$ is known as an index of Lyapunov exponent [20-21]. Accordingly, we can write that

$$|F(x_0 + \varepsilon) - F(x_0)| \approx \varepsilon e^{\lambda(x_0)}, \tag{59}$$

$$|F^2(x_0 + \varepsilon) - F^2(x_0)| \approx \varepsilon e^{\lambda(x_0)} \cdot e^{\lambda(x_0)} = \varepsilon e^{2\lambda(x_0)}, \tag{60}$$

$$|F^3(x_0 + \varepsilon) - F^3(x_0)| \approx \varepsilon e^{2\lambda(x_0)} \cdot e^{\lambda(x_0)} = \varepsilon e^{3\lambda(x_0)}, \dots, \tag{61}$$

$$|F^t(x_0 + \varepsilon) - F^t(x_0)| \approx \varepsilon e^{t\lambda(x_0)}. \tag{62}$$

From the last expression Eq.(62) we get

$$e^{t\lambda(x_0)} \approx \frac{|F^t(x_0 + \varepsilon) - F^t(x_0)|}{\varepsilon}, \tag{63}$$

$$t\lambda(x_0) \approx \ln \frac{|F^t(x_0 + \varepsilon) - F^t(x_0)|}{\varepsilon}, \tag{64}$$

$$\lambda(x_0) \approx \frac{1}{t} \ln \frac{|F^t(x_0 + \varepsilon) - F^t(x_0)|}{\varepsilon}. \tag{65}$$

Passing to the limit at $\varepsilon \rightarrow 0$ and $t \rightarrow \infty$ we get the correct formal expression for $\lambda(x_0)$:

$$\lambda(x_0) = \lim_{t \rightarrow \infty} \left(\frac{1}{t} \ln \lim_{\varepsilon \rightarrow 0} \frac{|F^t(x_0 + \varepsilon) - F^t(x_0)|}{\varepsilon} \right) = \lim_{t \rightarrow \infty} \left(\frac{1}{t} \ln \left| \frac{dF^t(x)}{dx} \right|_{x=x_0} \right). \tag{66}$$

Now we use the chain rule:

$$\frac{dF^2(x)}{dx} \Big|_{x=x_0} = \frac{dF(F(x))}{dx} \Big|_{x=x_0} = \left(\frac{dF(F(x))}{dF(x)} \cdot \frac{dF(x)}{dx} \right) \Big|_{x=x_0} = F'(x_1) \cdot F'(x_0), \tag{67}$$

$$\frac{dF^3(x)}{dx} \Big|_{x=x_0} = \frac{dF(F^2(x))}{dx} \Big|_{x=x_0} = \left(\frac{dF(F^2(x))}{dF^2(x)} \cdot \frac{dF^2(x)}{dx} \right) \Big|_{x=x_0} = F'(x_2) \cdot F'(x_1) \cdot F'(x_0), \dots, \tag{68}$$

$$\frac{dF^t(x)}{dx} \Big|_{x=x_0} = \prod_{i=0}^{t-1} F'(x_i). \tag{69}$$

Finally, we can use two forms of index of Lyapunov exponent:

$$\lambda(x_0) = \lim_{t \rightarrow \infty} \left(\frac{1}{t} \ln \prod_{i=0}^{t-1} |F'(x_i)| \right) \tag{70}$$

or

$$\lambda(x_0) = \lim_{t \rightarrow \infty} \left(\frac{1}{t} \sum_{i=0}^{t-1} \ln |F'(x_i)| \right). \tag{71}$$

Distribution of Lyapunov index characterizes the behaviour of chaotic dynamics as well as various forms of stabilization or synchronization [15]. Positive value of Lyapunov index indicates chaotic behaviour of the sequence according to sensitive dependence on initial x_0 . A negative value of it indicates absence of chaotic dependence on initial x_0 .

General question could be formulated as follows: is a given system periodic or “chaotic”? And if so, how chaotic? [22, p.293]. Chaotic behaviour of dynamic system could be estimated using index of Lyapunov characteristic exponent $\lambda(r)$ which gives the rate of exponential divergence related to the initial condition. Distribution of Lyapunov index express the behaviour of period-double route which tends to chaos manner. For discrete analog of Verhulst equation when $F(x)=rx(1-x)$ we have three situations: a) $\lambda < 0$ in periodic regime, b) $\lambda = 0$ period-doubling (at bifurcation point), c) $\lambda > 0$ in chaotic regime.

Distribution of index of Lyapunov exponent is just one type of spectra which can be associated with a linear, time-varying system [23, p.730].

2. Advanced tool QUATTRO-20

For learning purposes, program package an advanced tool QUATTRO-20 [17] was created and tested. Classical recurrent sequence generated using Discrete Analogue of Verhulst equation, $x_{t+1}=F(x_t)$, where $F(x)=rx(1-x)$ was used as a model sequence. Second composition $F^2(x)$, third composition $F^3(x)$, fourth composition $F^4(x)$ and first derivatives of $F(x)$, $F^2(x)$, $F^3(x)$, $F^4(x)$ with respect to x were considered and visualized.

Main goals of QUATTRO-20 could be formulated as follow:

- i) estimation of the quantity and quality of recurrent sequence in digital and graphical form;
- ii) estimation of convergence or chaos behaviour of recurrent sequence.

Several visualization methods such as Bifurcation diagram, distribution of index of Lyapunov exponent and CobWeb plot (see Table 1) are included in the package.

Table 1. *QUATTRO-20*. Visualization methods.

N	Routine	Formula	Algorithm
1.	Bifurcation diagram	Eq.(2)	Table 2
2.	Map of first derivative	-	Table 3
3.	Distribution of Lyapunov index	Eq.(71)	Table 4
4.	Cobweb plot	-	Table 5
5.	Graphical solution	Eq.(19)	-
6.	Generation of recurrent sequence	Eq.(2)	Table 2

Bifurcation diagram. Fig. 3 represents the main window of *QUATTRO-20* which contains related dependencies: Bifurcation diagram for $x_{t+1}=rx_t(1-x_t)$ (top left), distribution of corresponding Lyapunov exponent (bottom left) (argument $r \in (0; 4)$ in both cases). CobWeb plot corresponds the cut of Bifurcation diagram when $r=3.6$ (top right). For easy visualization, state marker (red vertical line) at $r=3.6$ is presented in Bifurcation diagram and distribution of Lyapunov exponent. Graphical solution (top right) of Eq. $x=3.6 \cdot x(1-x)$ related to CobWeb plot is presented in numerical form (bottom right): $x_1^*=0, x_2^*=0.723$. Fig. 4 represents partial case of Fig. 3, when argument $r \in (3.79; 3.91)$ and state marker is fixed at $r_{fix}=3.846$.

Bifurcation diagram, also Finite-State diagram (previous term presented in [10, 18]), also Feigenbaum plot (pioneering term from 7th decade of XX century, used in [10, 14]) enable the visualization of bifurcation theory. Generally, Bifurcation diagram must represent distribution of the attractor points x^* on parameter r expressed in analytical dependencies. The solution x_1^* is the fixed point attractor for $0 < r < 1$, x_2^* - for $1 < r < 3$ - see Eq.(20). Solutions $x_3^{*(2)}$ and $x_4^{*(2)}$ are the periodic attractors for $3 < r < 3.45$ - see Eq.(35). "Pure" expressed Bifurcation diagram is presented in Fig. 2. For exact solution of Eq. $x=F^4(x)$ at interval $3.45 < r < 3.54$ is necessary to solve the 16th-order polynomial equation. Unfortunately, this solution is very complicated, resource-wasting and difficult. Then, for interval $3.54 < r < 4.0$ is necessary to solve equations containing high-order polynomials. This exact routine could be replaced using approximation technique only.

For any recurrent sequence, several algorithms could be realized: for example, Feigenbaum plot presented in [10, p.652], [24] etc. Table 2 represents simplified algorithm *BifurcationDiagram* presented in Java style which was realized in *QUATTRO-20*. Several values must be passed to method *BifurcationDiagram*: $x_0, iT, rFrom, rUntil, rStep$. Initial value x_0 could be established by user from interval (0; 1). Practically, values very close to 0 or very close to 1 are not acceptable due to necessity to pass the big number of initial items. We used default value $x_0=0.3$.

Number of iterations iT allows to generate the requested amount

Table 2. *QUATTRO-20*. Algorithm *BifurcationDiagram*.

```

void BifurcationDiagram(double x0, int iT,
    double rFrom, double rUntil, double rStep)
{
    double xCur, xNext, rr;
    for (rr=rFrom; rr<=rUntil; rr+=rStep)
    {
        xCur = x0;
        for (int i=0; i<iT; i++)
        {
            xNext = rr * xCur * (1.0 - xCur);
            xCur = xNext;
        }
    }
}

```

Table 3. *QUATTRO-20*. Algorithm *FIMap*.

```

void FIMap(double x0, int iT,
    double rFrom, double rUntil, double rStep)
{
    double xCur, xNext, xDer, rr;
    for (rr=rFrom; rr<=rUntil; rr+=rStep)
    {
        xCur = x0;
        for (int i=0; i<iT; i++)
        {
            xDer = rr * (1.0 - 2.0 * xCur);
            xNext = rr * xCur * (1.0 - xCur);
            if (( 0.0<xDer)&&(xDer<1.0))
                DrawPoint (rr, xNext, "red");
            else if ((-1.0<xDer)&&(xDer<0.0))
                DrawPoint (rr, xNext, "green");
            else
                DrawPoint (rr, xNext, "blue");
            xCur = xNext;
        }
    }
}

```

of sequence items to receive the distribution of stable manner as well as chaotic. Default value is equal to $iT=5000$ but could be increased according to user needs.

Parameter r could be presented in interval: from initial value $0 < rFrom < 4$ until final value $0 < rUntil \leq 4, rFrom < rUntil$. Step $rStep$ predetermines the quantity of data saturation in Bifurcational diagram and is related to the width of interval ($rFrom; rUntil$). Default value $rStep=0.1$ could be decreased according to user needs.

Bifurcation diagram could be titled as some sort of fingerprints of recurrent sequence. We can see interval $r \in (0; 3.54)$ where small number of final states is present (one, two, four). Starting from $r=3.54$ up to $r=4.00$, number of final states rapidly increases with period doubling (chaotic states occur).

Map of first derivative. In addition, Bifurcation diagram was re-examined due to convergence condition [25]. It was interesting for us to get the domain in which the first derivative of F, F^2, F^3, F^4 with respect to x satisfies the following conditions:

$$\left| \frac{dF(x)}{dx} \right| < 1, \tag{72}$$

$$\left| \frac{dF^n(x)}{dx} \right| < 1, \quad n = 2, 3, 4. \tag{73}$$

Table 3 represents an algorithm *FIMap*. Several values must be passed to method *FIMap*: $x_0, iT, rFrom, rUntil, rStep$. First loop is devoted to parameter r which varies from $rFrom$ until $rUntil$ using step $rStep$. Second loop is devoted to iterations from 0 to iT (step 1). In inner loop, two loop values will be calculated:

- a) x_{next} using the current value x_{cur} , which represents an item of $F(x)$, according to Eq.(17) and
- b) x_{der} using the current value x_{cur} , which represents an item of first derivative of F , according to Eq.(22).

Using received values x_{der} , decision about point colouring in Bifurcation diagram must be made: for interval (0;1) - in red, for (-1;0) - green, else - blue. In case of F^2, F^3, F^4 , similar algorithms were used. For F^2, x_{next} argument will be calculated using Eq.(29), x_{der} - Eq.(33). For F^3, x_{next} argument will be calculated using Eq.(47), x_{der} - Eq.(49), For F^4, x_{next} argument will be calculated using Eq.(51), x_{der} - Eq.(52).

Fig. 5 represents the realization of convergence conditions: map of first derivative of $F(x), F^2(x), F^3(x), F^4(x)$ with respect to x (from top to bottom). Parameter $r \in (0, 4]$ with step 0.01 is presented

Table 4. *QUATTRO-20*. Algorithm *LE*.

```
double LE(double x0, int iT,
double rFrom, double rUntil, double rStep)
{
double xCur, xNext, xDer, xVal, rr;
double lambda, dSum;
for (rr=rFrom; rr<rUntil; rr+=rStep)
{
xCur = x0;
dSum=0.0;
for (int i=0; i<iT; i++)
{
xNext = rr * xCur * (1.0 - xCur);
xDer = rr * (1.0 - 2.0*xCur);
xVal = ln(abs(xDer));
dSum +=xVal;
xCur = xNext;
}
lambda = dSum / iT;
return lambda;
}
}
```

at horizontal axis and $x \in (0;1)$ on vertical axis. Red area represents the interval where values of corresponding derivative are positive and less than 1, green area – are negative and greater than -1 (for both case convergence condition is satisfied) and blue area – all the rest values (convergence condition is unsatisfied). Information about convergence was passed to the Fig. 6: Bifurcation diagram for $x_{t+1}=rx_t(1-x_t)$ was coloured according to value of convergence for $F(x), F^2(x), F^3(x), F^4(x)$. Figs. 7,8 represent partial case of Figs. 5,6, when argument interval was squeezed: $r \in (3.4;4.0)$.

Inner structure of Bifurcation diagram could be analysed using additional approaches. The distribution of points is inhomogeneous, it is possible to notice several areas where the concentration of points is higher. Fig. 8 represents the intersection of two chaotic branches at special point whose coordinates are as follows: $r \approx 3.68, x \approx 0.73$. This particular point is called the first Misiurewicz point [26]. The value of calculated Misiurewicz point is equal to A , and corresponding ordinate X_A :

$$A = 3.67857351042832226... \quad (74)$$

$$X_A = 0.728155493653961819... \quad (75)$$

Distribution of Lyapunov index. Chaotic behaviour of dynamic system could be estimated using Lyapunov index $\lambda(x_0)$ which gives the rate of exponential divergence related to the initial condition - Eq.(71). For detailed explanation, see [21, p.96] Table 4 represent an algorithm *LE* which was realized in *QUATTRO-20*. Several values must be passed to method *LE*: $x_0, iT, rFrom, rUntil, rStep$. Actually, Eq.(71) represents summation when parameter $t \rightarrow \infty$. Practically, parameter t could be reduced to 100..500. Sum of natural logarithm of absolute value of x_{der} at current x_{cur} will be divided by iT value, number of iterations. Distribution of Lyapunov index $\lambda(x_0)$ in requested interval of r is presented in Fig. 3 (bottom left) partial case in Fig. 4 (bottom left).

For stable fixed points (periodic mode) at $r \in (0;3.45), \lambda(x)$ value is negative. For special points $r=1$ and $r=3, \lambda(x) \rightarrow 0$. Bifurcation point (period-doubling mode) could be established using condition: $\lambda(x)=0$. For $r \in (3.45; 4.00), \lambda(x)$ is positive (chaotic mode). The distribution of the Lyapunov index complements the evaluation of the type of recurrent sequence which was done using the Bifurcation diagram only. Three modes: chaotic, period-doubling and periodic - can be evaluated regardless of the precision of the calculation technique [27].

CobWeb plot. A CobWeb plot, or Verhulst diagram (previous term) represents an graphical method to find the fixed points of sequence. Problem could be formulated as follows. Fixed points may not be found analytically for some maps due to different circumstances [2]. In such case, CobWeb diagram is useful to determine the fixed points in the xy plane and their convergence characters [28, p. 417]. Construction and interpretation of CobWeb plot is widely described in [11].

Let us consider two functions $y=x$ and $y=rx(1-x)$. CobWeb plot will be generated for fixed r . Table 5 represents an algorithm *CobWeb*. Several values must be passed to method *CobWeb*: x_0, rr, iT . Number of iterations, iT , previously defined by user (from several hundreds to several thousands), allow to generate the requested number of point pairs (x,y) . Each iteration contains four points, which allow to draw two vertical lines and two horizontal lines in presented order.

Let us consider the initial pair (x_0, y_0) as starting point. Let $x_0=0.3$ (default value), let $y_0=0$ (start from x axis). One loop of iteration contains four routines:

- 1) calculation of value $y_1=F(x_0)$, drawing a vertical line from $(x_0; y_0)$ to the intersection with the parabola $(x_0; y_1)$;
- 2) passing of value $x_1=y_1$, drawing a horizontal line from $(x_0; y_1)$ to the intersection with line $(x_1; y_1)$;
- 3) calculation of value $y_0=F(x_1)$, drawing a vertical line from $(x_1; y_1)$ to the intersection with the parabola $(x_1; y_0)$;
- 4) passing of value $x_0=y_0$, drawing a horizontal line from $(x_1; y_0)$ to the intersection with line $(x_0; y_0)$.

Figs. 3,4 represent CobWeb plots at fixed r which corresponds the current distributions of states in Bifurcation diagram. Program *QUATTRO-20* allows to draw all generated lines (from 0 until iT) as well as requested lines only (from $iT0$ until iT). Fig. 4 represents CobWeb plot where mentioned situation was realized: only part of final iterations are significant to estimate non-chaotic closed-to-order mode of distribution. The red vertical line on the Bifurcation diagram (at $r=3.6$) corresponds to the oscillation section on the CobWeb graph. Iterations from the requested interval [100, 400] are shown in red, another interval [1, 100] is shown in white (completely invisible).

Graphical solution. CobWeb plot could be treated as the graphical tool for solution of Eq.(19). Figs. 3,4 represent intersection of two graphs: linear function $y=x$ and parabola $y=F(x)$, when $F(x)=rx(1-x)$ at fixed r (top right). Coordinates of two intersection points are presented numerically (bottom right):

$x_1^*=0, x_2^*=0.723$ at $r=3.6$, see Fig. 3,

$x_1^*=0, x_2^*=0.740$ at $r=3.846$, see Fig. 4.

Table 5. *QUATTRO-20*. Algorithm *CobWeb*.

```
void CobWeb(double x0, double rr, int iT)
{
double xCur0, yCur0, xCur1, yCur1;
xCur0= x0; yCur0=0.0;
for (int i=0; i<iT; i++)
{
yCur1 = rr * xCur0 * (1.0 - xCur0);
DrawVerLine(xCur0, yCur0, yCur1);
xCur1 = yCur1;
DrawHorLine(xCur1, xCur0, xCur1);
yCur0 = rr * xCur1 * (1.0 - xCur1);
DrawVerLine(xCur1, yCur1, yCur0);
xCur0 = yCur0;
DrawHorLine(yCur0, xCur1, xCur0);
}
}
```

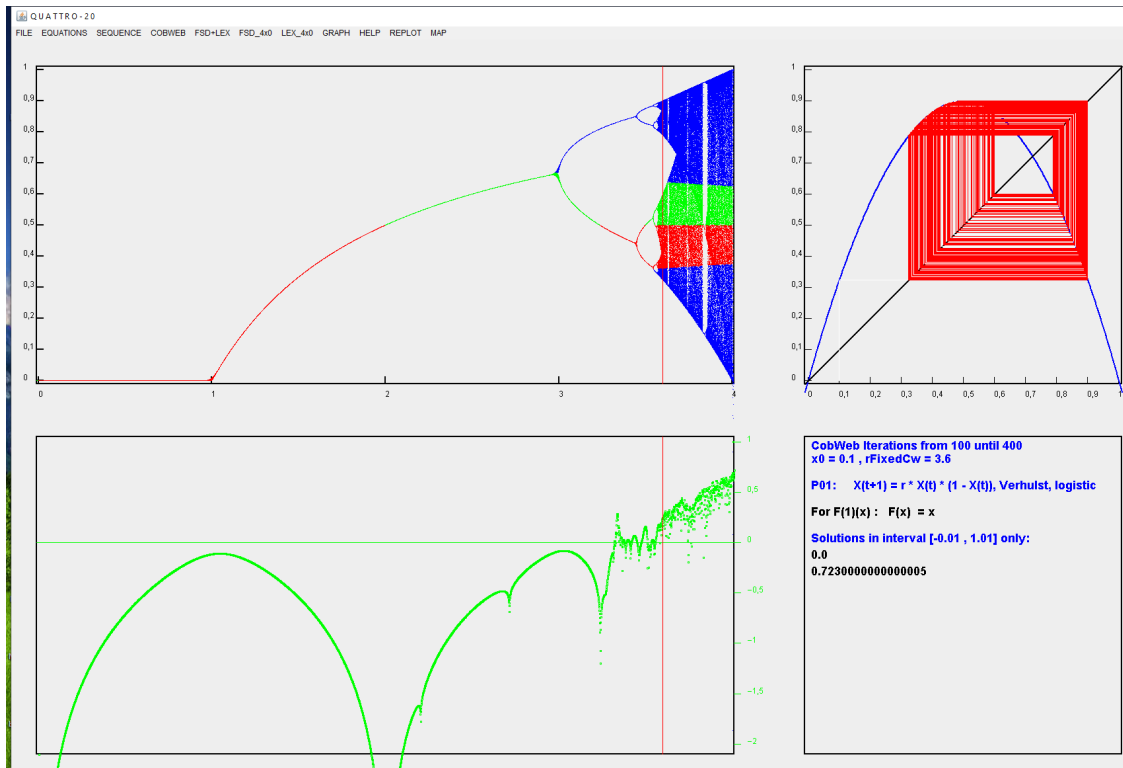



Fig. 3. *QUATTRO-20*. Main window for dependencies: Bifurcation diagram for sequence $x_{t+1} = r \cdot x_t(1-x_t)$ (top left), distribution of corresponding Lyapunov index (bottom left) when $r \in (0; 4)$. State marker (red vertical line) at $r=3.6$. CobWeb plot corresponds state distribution when $r=3.6$ (top right). Graphical solution of Eq. $x = 3.6 \cdot x(1-x)$ (top right) related to CobWeb plot is presented in numerical form (bottom right).

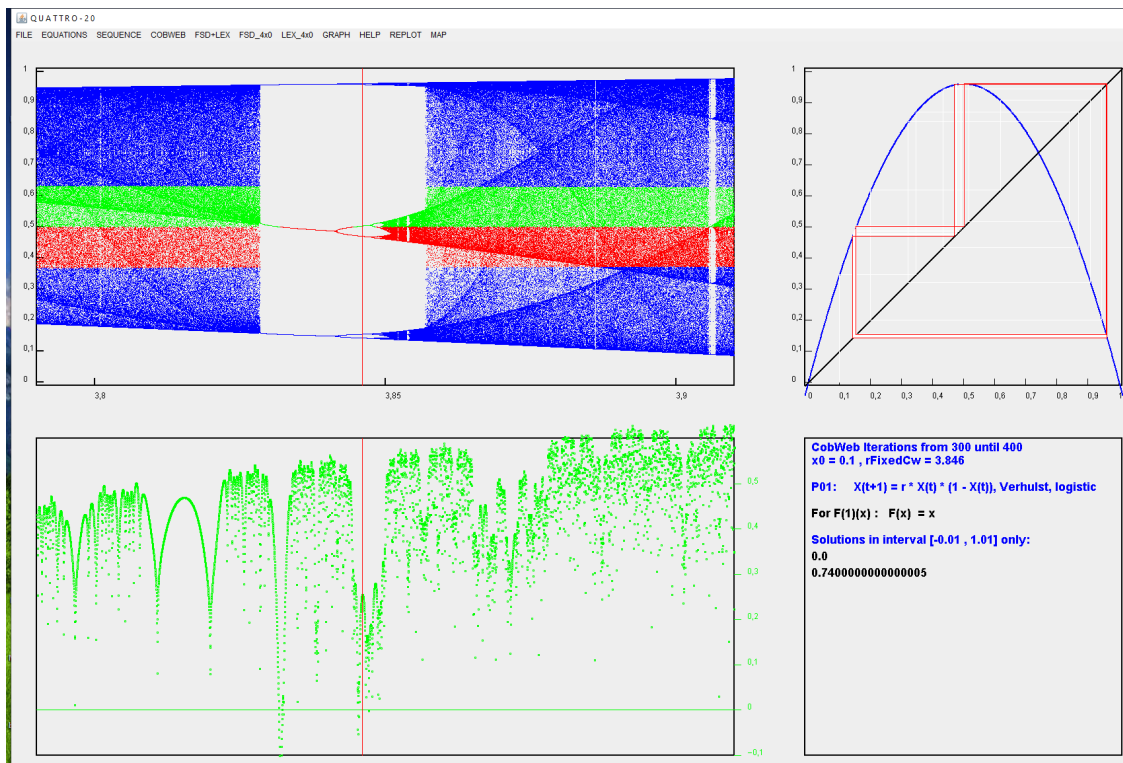


Fig. 4. *QUATTRO-20*. Partial case of Fig. 3: $r \in (3.79; 3.91)$. State marker (red vertical line) at $r=3.846$. CobWeb plot corresponds state distribution when $r=3.846$ (top right). Graphical solution of Eq. $x = 3.6 \cdot x(1-x)$ (top right) related to CobWeb plot is presented in numerical form (bottom right).

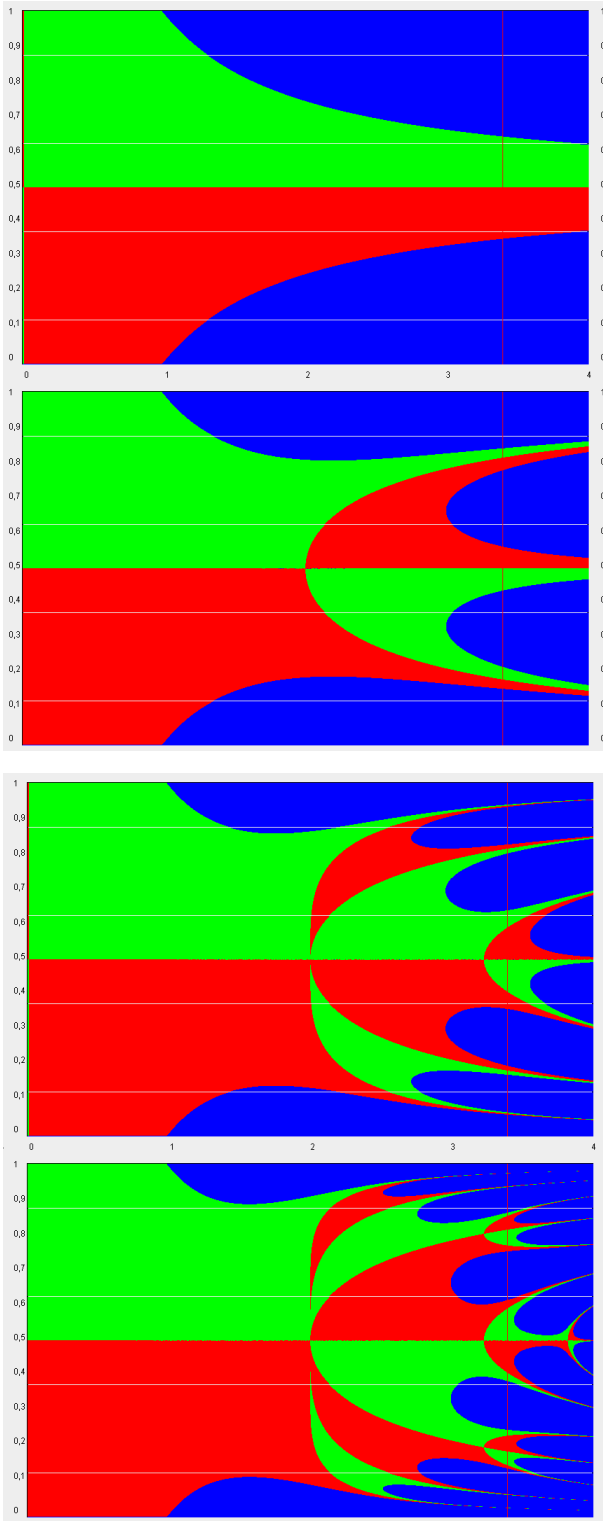


Fig. 5. *QUATTRO-20*. Realization of convergence conditions. Map of first derivative of $F(x)$, $F^2(x)$, $F^3(x)$, $F^4(x)$ with respect to x (from top to bottom). $r \in (0;4)$ at horizontal axis and $x \in (0;1)$ on vertical axis. Red area represents the values of derivative in interval $[0,1]$, green - $[-1,0)$ (convergence condition is satisfied) and blue - all the rest (convergence condition is not satisfied).

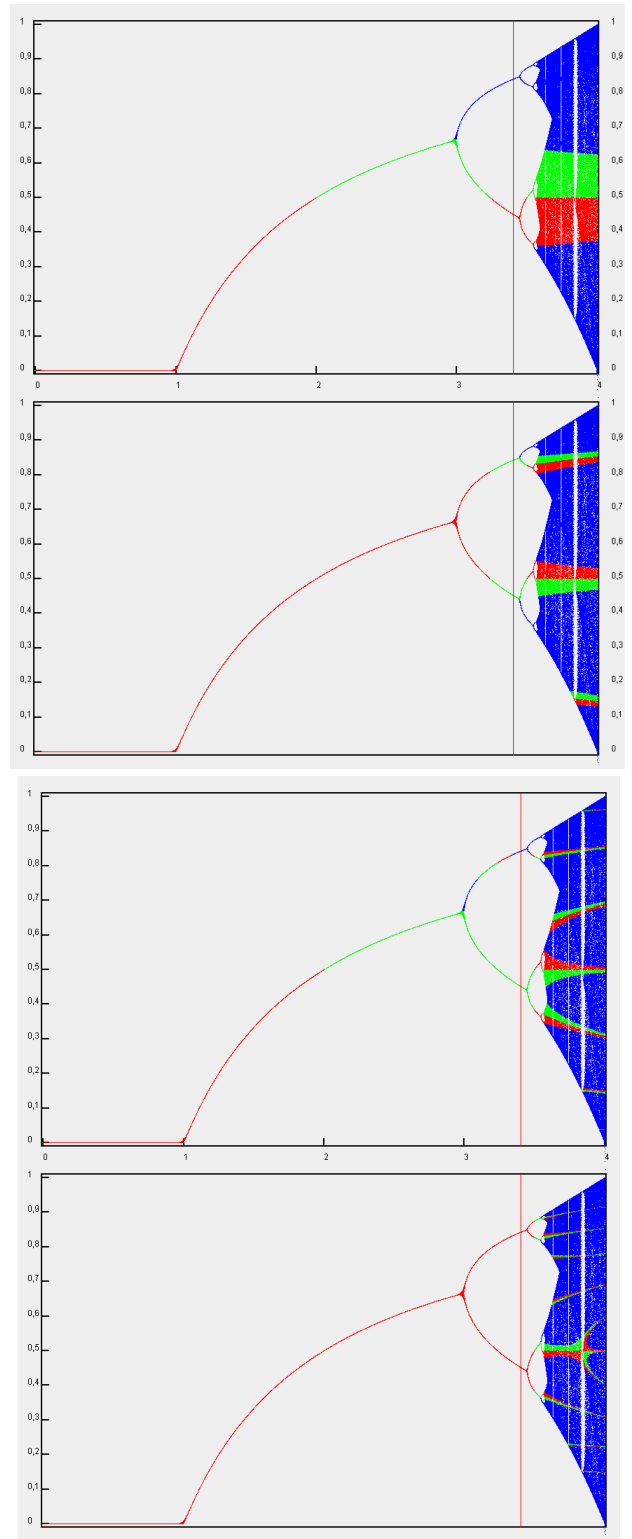


Fig. 6. *QUATTRO-20*. Sequence $x_{t+1} = r x_t (1 - x_t)$. Bifurcation diagram coloured according to condition of convergence for first derivative of $F(x)$, $F^2(x)$, $F^3(x)$, $F^4(x)$ with respect to x (from top to bottom), see Fig. 5.

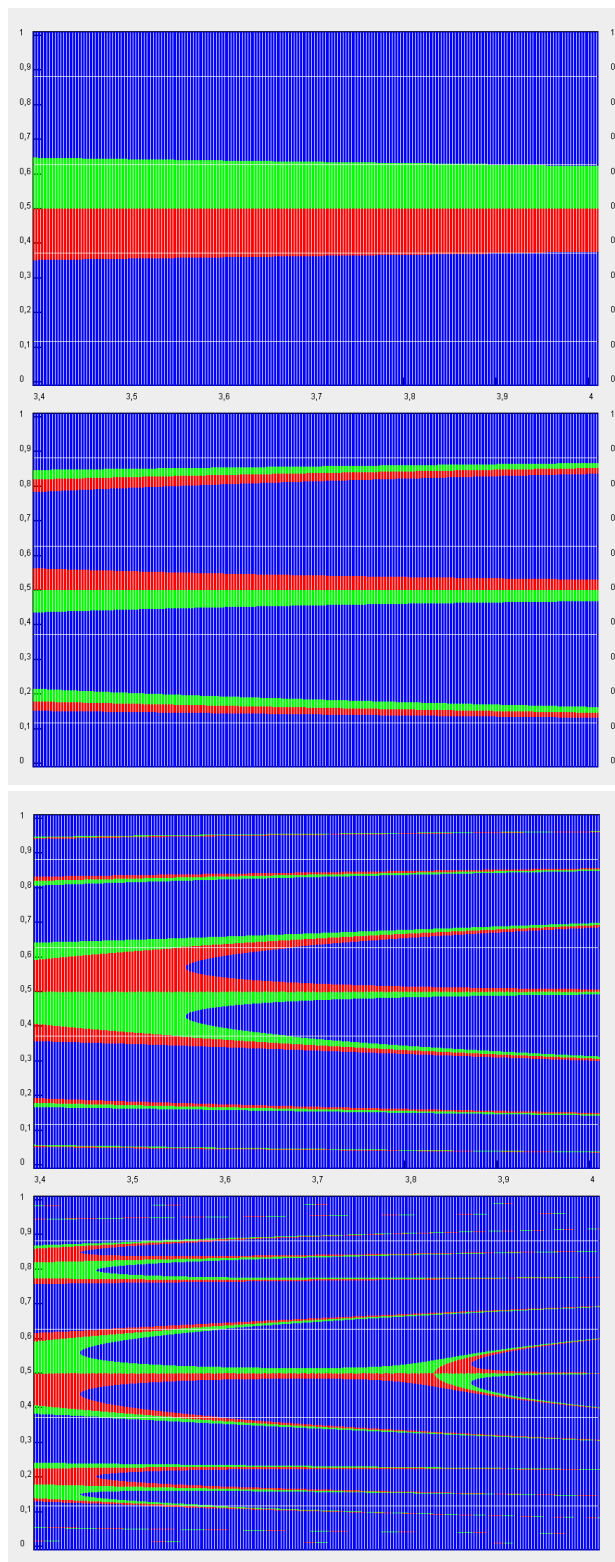


Fig. 7. *QUATTRO-20*. Realization of convergence conditions. Partial case of Fig. 5. Map of first derivative of $F(x)$, $F^2(x)$, $F^3(x)$, $F^4(x)$ with respect to x (from top to bottom). $r \in [3.4; 4]$ at horizontal axis and $x \in [0; 1]$ on vertical axis. Red area represents the values of derivative in interval $[0, 1]$, green - $[-1, 0)$ (convergence condition is satisfied) and blue - all the rest (convergence condition is not satisfied).

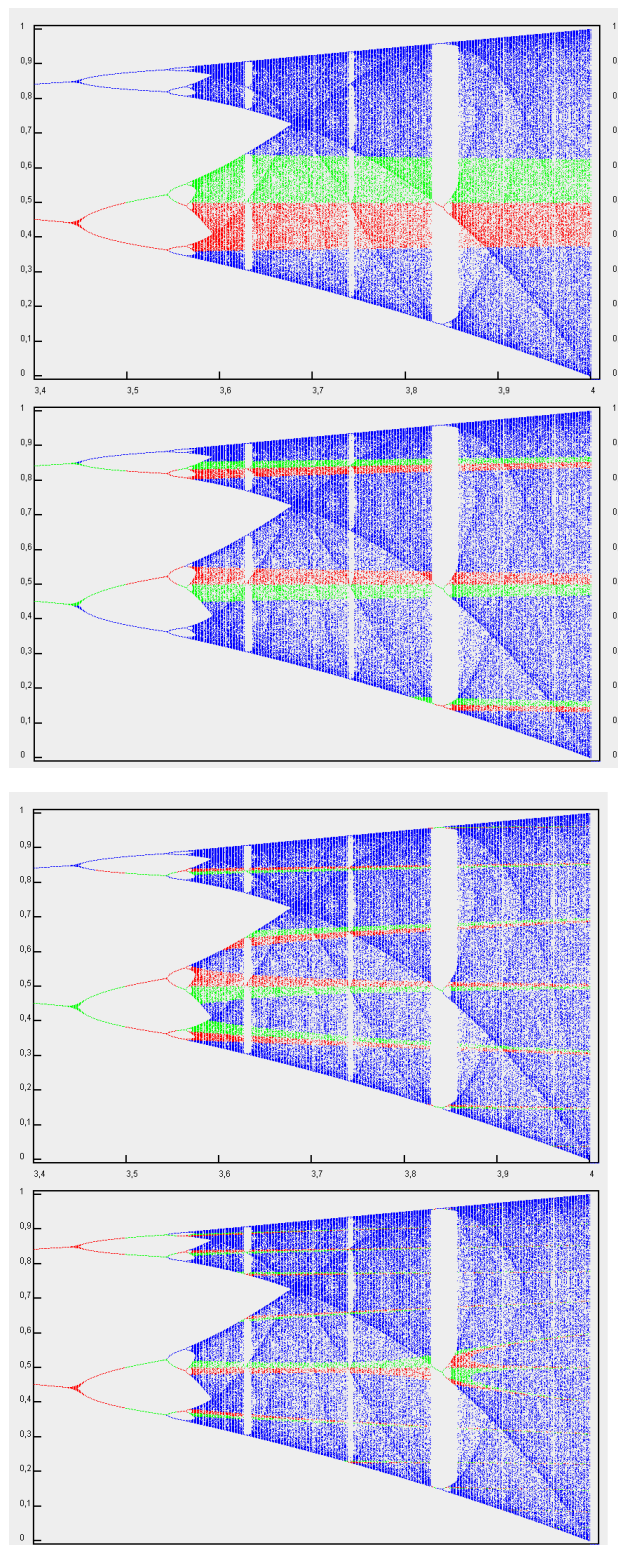
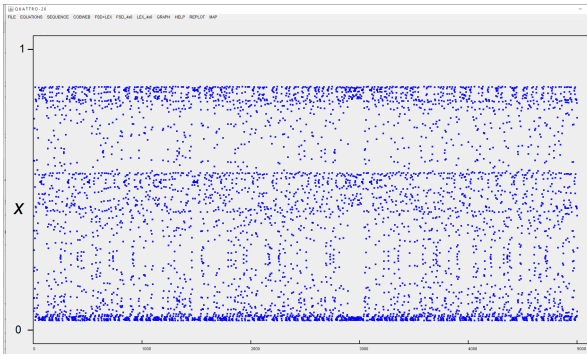
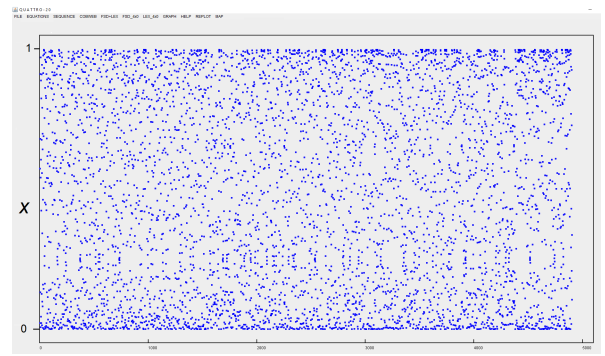


Fig. 8. *QUATTRO-20*. Partial case of Fig. 5. $r \in (3.4; 4)$. Bifurcation diagram for sequence $x_{t+1} = r x_t (1 - x_t)$ coloured according to condition of convergence for first derivative of $F(x)$, $F^2(x)$, $F^3(x)$, $F^4(x)$ with respect to x (from top to bottom).



a) $r=3.860$



b) $r=4.000$.

Fig. 9. *QUATTRO-20*. xy distribution of sequence $x_{t+1}=rx_t(1-x_t)$ at fixed r . For both cases $x_0=0.3$, 5000 iterations.

Generation of the recurrent sequence. According to requests of users, some necessity to estimate chaotic behaviour of the recurrent sequence must be realized using simple "show as it is" technique.

Historically, the numerical analysis of recurrent sequences has been recognized as a very difficult routine task. For example, in [13], small and big perturbations of parameters of dynamic system was provided manually, using standard growth model. Due to that, all graphical visualization techniques are wellcome.

In *QUATTRO-20*, generation of big amount of data was realized using previously described algorithm of Bifurcation diagram presented in Table 2. Fig. 9 represent the xy distribution of recurrent sequence $x_{t+1}=rx_t(1-x_t)$ at fixed r . For both cases iteration starts from the same value $x_0=0.3$, and 5000 iterations were provided. Fig. 9a shows far-away from chaotic distribution ($r=3.860$) in interval approximately (0.05; 0.9) but not in (0;1). Fig. 9b shows chaotic distribution ($r=4.000$) in interval (0;1). Recurrent sequence when $r \rightarrow 4$ do not always converge. This result could be checked using Bifurcation diagram - see Fig 3,4. All generated sequences in ASCII form could be output to file for additional analysis using statistical packages.

Input parameters. Initially, all input parameters are presented as routine parameters (by default) which allow receiving output of previously defined task. Fig. 10 represents the screenshot of parameter window which is necessary to establish or to correct for the routine of recurrent sequence generation. For example, $x_0=0.3$, $r_{fixed}=3.86$. For recurrent sequence generation, number of iterations is equal to $iT=5000$. For output to screen, requested interval (horizontal coordinates) from $iT_{from}<5000$ until iT could be used.

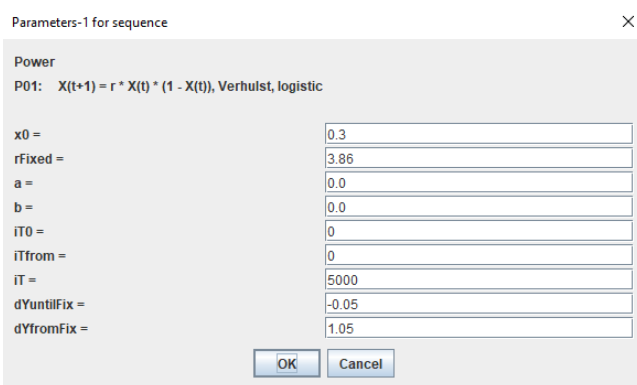


Fig. 10. *QUATTRO-20*. Parameters for recurrent sequence generation.

Also requested interval (vertical coordinates) from $dY_{fromFix}=-0.05$ until $dY_{untilFix}=1.05$ could be used or could be changed. All initial parameters are presented for realization of digital or graphical output without significant wasting of computer resources. Next, user can change the parameters due to any requests (initial value x_0 in interval $x \in (0;1)$, number of iterations, parameter r etc).

Fig. 11 represents the screenshot of parameter windows which is necessary to establish or to correct for plotting Bifurcation diagram, distribution of Lyapunov index and CowWeb plot. Previously, all default parameters are presented at the initial stage of start. For example, $x_0=0.3$, parameter r must be established in some interval: $R_{from}=3.4$, $R_{until}=4.01$, step of changes $R_{step}=0.001$. For recurrent sequence generation, number of iterations is equal to $iTT=400$. For generation of recurrent sequence at current r , requested interval (horizontal coordinates) from $iTT_{from}=100$ to iTT must be used. In all cases, iTT_{from} must be established as non-zero parameter (always is necessary to avoid the initial part of recurrent sequence). Requested interval (vertical coordinates for Bifurcation diagram) from $dY_{from}=-0.01$ until $dY_{until}=1.01$ could be used or could be changed. Also requested interval (vertical coordinates for distribution of Lyapunov plot) from $dY_{fromLE}=-2.1$ until $dY_{untilLE}=1.05$ could be used or could be changed. Next, user can change the parameters due to any requests.

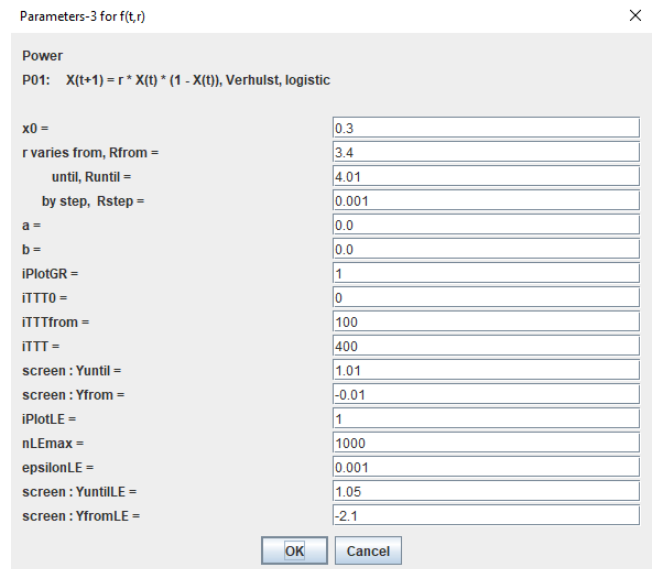


Fig. 11. *QUATTRO-20*. Parameters for Bifurcation diagram, distribution of Lyapunov index and CowWeb plot.

3. Main results and discussion

The assessment should be divided into two parts.

Firstly, the analysis of the behaviour of recurrent sequence $x_{t+1}=rx_t(1-x_t)$ for $x \in (0,1)$ and for $r \in (0,4]$ with a different step can be done - see Figs. 3, 4. Bifurcation diagram can be drawn for dynamic system to establish the transition conditions: from periodic behaviour to chaotic behaviour. Bifurcation diagram in vertical direction is related to the distribution of Lyapunov index (for the same value of parameter r), otherwise, Bifurcation diagram in horizontal direction is related to the CobWeb plot (for the same value of $x \in (0;1)$).

Secondly, switching between several modes - periodic, chaotic and period-doubling - must be established from Bifurcation diagram. There is a number of functions approaching the chaos type sequence *via* period doubling. Conclusion about switching between modes must be verified and enforced by analysing the distribution of Lyapunov index. Generation of chaotic states is related to the Lyapunov index λ , which value increases from negative to positive. For periodic modes, mentioned value is negative.

Establishing of chaos generation mode using parameter $r=4.0$ allows us to receive the sequence of pseudo-random numbers, which could be used in any place where unpredictability is welcome. [29]. Small changes in the initial value generate the big differences between predicted or guessed values. *QUATTRO-20* could be used for generation of pseudo-random numbers (not for cryptography, for learning purposes only) and following numerical output to electronic storage. User can estimate the uniform or pseudo-uniform distribution of recurrent sequence members from diagrams - see Figs. 9a,b. In [29], a critical evaluation of several popular algorithms for generation the pseudo-random numbers is presented. Maps of first derivative of $F(x)$, $F^2(x)$, $F^3(x)$, $F^4(x)$ with respect to x (see Fig. 5) give the additional information about behaviour of recurrent sequence. For $F^2(x)$, $F^3(x)$, $F^4(x)$ dependencies, first

active point is presented at $r_1=2.0$, second - at $r_2=3.2$ (switching between red and green colour means switching between negative and positive values of the first derivative with respect to x). This region of interest is far-away from chaotic region of recurrent sequence (where $r>3.56$, see Fig. 6).

Conclusions

Following practical results were obtained as presented below.

Advanced tool *QUATTRO-20* for estimation the properties of recurrent sequence was created, tested and approved. *QUATTRO-20* allows comparing the various aspects of chaotic system dynamics in the framework of graphical models.

Traditional graphic models such as Bifurcation diagram, distribution of Lyapunov index, CobWeb plot (together with graphical solution $x=F(x)$) were used in the common graphical interface. Additional approaches such as maps of first derivative of $F(x)$, $F^2(x)$, $F^3(x)$, $F^4(x)$ with respect to x were realized for estimation purposes.

Generation of xy recurrent sequence of requested amount and following numerical output to electronic storage was realized.

Authors' contributions

Jelena Kozmina formulated general idea, presented critical literature review, derived mathematical formulas and validated results. Alytis Gruodis created programming package *QUATTRO-20* (source code in Java), realized the graphical implementation and prepared description of program. Both authors reviewed and approved the final manuscript.

Conflicts of interest

Authors declared at they have no conflicts of interest.

References

- Cencini, M.; Cecconi, F; Vulpiani, A. (2009) Chaos. From Simple Models to Complex Systems - World Scientific, Singapore, 2009.
- Klages, R. (2008) Introduction to Dynamical Systems. Lecture Notes for MAS424/MTHM021. Version 1.2 - Queen Mary, University of London, 2008.
- Quinn, T. (2013) Population Dynamics. - In: Encyclopedia of Environmetrics. 2nd Ed. - John Wiley & Sons, Ltd. - <https://doi.org/10.1002/9780470057339.vap028>.
- Strogatz, S. H. (2015) Nonlinear dynamics and chaos: with applications to physics, biology, chemistry and engineering. - CRC Press, 2015.
- Uzokov, O.X. (2020) Chaos as the Basis of Order. Entropy as Measures of Chaos - *International Journal of Advanced Research in Science, Engineering and Technology* 7(12) (2020) 16149-16154.
- Bertels, K.; Neuberger, L.; Vassiliadis, S.; Pechanek, D. (2001) On Chaos and Neural Networks: The Backpropagation Paradigm - *Artificial Intelligence Review* 15(2001)165-187.
- Bacaer, N. (2011) A Short History of Mathematical Population Dynamics. - Springer-Verlag London Limited, 2011. - <https://doi.org/10.1007/978-0-85729-115-8-6>.
- May, R. (1974) Biological Populations with Nonoverlapping Generations: Stable Points, Stable Cycles, and Chaos - *Science* 186(1974)645-7. - <https://doi.org/10.1126/science.186.4164.645>.
- Lorenz, E. N. (1990) Can chaos and intransitivity lead to interannual variability? - *Tellus* 42A (1990)378-389. - <https://doi.org/10.1034/j.1600-0870.1990.t01-2-00005.x>
- Heinz-Otto Peitgen, Hartmut Jurgens, Dietmar Saupe (1992) Chaos and Fractals. New Frontiers of Science. - Springer-Verlag.
- Kozmina, Y. (2018) Discrete Analogue of the Verhulst Equation and Attractors. Methodological Aspects of Teaching - *Innovative Infotechnologies for Science, Business and Education* 1(24) (2018) 3-12.
- Petropoulou, E. N.(2010) A Discrete Equivalent of the Logistic Equation - *Advances in Difference Equations* 2010 (2010) 57073-57088 - <https://doi.org/10.1155/2010/457073>.
- Kalman, D. (2023) Verhulst Discrete Logistic Growth - *Mathematics Magazine* 96:3 (2023) 244-258 - <https://doi.org/10.1080/0025570X.2023.2199676>.
- Conejero, J.A.; Garibo-i-Orts, O.; Lizama, C. (2023) Inferring the fractional nature of Wu Baleanu trajectories. - *Nonlinear Dynamics* 111(2023) 12421–12431 - <https://doi.org/10.1007/s11071-023-08463-1>.
- Pikovsky A., Rosenblum M., and Kurths J. (2001) Synchronization. A Universal Concept in Nonlinear Sciences - Cambridge: Cambridge University Press.
- Afsar, O.; Eroglu, D.; Marwan, N.; Kurths, J. (2015) Scaling behaviour for recurrence-based measures at the edge of chaos. - *Europhysics Letters* - 112(2015)10005 - <https://doi.org/112.10.1209/0295-5075/112/10005>.

17. Kozmina, J.; Gruodis A. (2020) *QUATTRO-20* - WinApi program. - <https://github.com/Alytis/QUATTRO-20>.
18. Alligood, K. T.; Sauer, T. D.; Yorke, J. A. (1996) *Chaos. An introduction to dynamical systems.*- Springer-Verlag, 1996.
19. Holmgren, R.A. (2000) *A first course in discrete dynamical systems.* Sec. Edition - Springer-Verlag, 2000.
20. Schuster, H. G.; Just, W. (2005) *Deterministic Chaos. An Introduction* - WILEY-VCH Verlag GmbH & Co. KGaA, Weinheim, 2005.
21. Robinson, C. (1995) *Dynamical systems. convergence, symbolic dynamics, and chaos.*- CRC Press, 1995.
22. Cvitanovic, P.; Artuso, R.; Mainieri, R.; Tanner, G.; Vattay, G. (2011) *Chaos: Classical and Quantum. Volume I: Deterministic Chaos - Gone With the Wind* press, Atlanta, 2011
23. Wiggins, S. (2000) *Introduction to Applied Nonlinear Dynamical Systems and Chaos. Second Edition.* - Springer, 2000. - 860 p.
24. Gesmann, M. (2012) Logistic map: Feigenbaum diagram in R. - <https://magesblog.com/post/2012-03-17-logistic-map-feigenbaum-diagram/>.
25. Kozmina, Y.; Gruodis, A. (2020) QUATTRO-20: advanced tool for estimation of the recurrent sequences - In: 18th International Conference "Information Tehnologies and Management", April 23-24, 2020, ISMA University of Applied Science, Riga, Latvia.
26. Misiurewitz, M. (1981) Absolutely continuous measures for certain maps of an interval - *Publications mathématiques de l'I.H.É.S.* 53 (1981) 17-51. - http://www.numdam.org/item?id=PMIHES_1981_53_17_0.
27. Huberman, B. A.; Rudnick, J. (1980) Scaling Behavior of Chaotic Flows - *Phys. Rev. Lett.* 45 (1980) 154. - <https://doi.org/10.1103/PhysRevLett.45.154>.
28. Layek, G. (2015) *An Introduction to Dynamical Systems and Chaos.* - <https://doi.org/10.1007/978-81-322-2556-0>.
29. Kozmina, Y.; Gruodis, A. (2019) Number generation based on the chaotic sequences - In: The 17th International Scientific Conference "Information Technologies and Management - 2019", April 25-26, 2019, ISMA, Riga, Latvia - *Nano Technologies and Computer Modelling* (2019)17-18.